

# Chemically modified Egyptian montmorillonite clay with mercaptopropyl trimethoxysilane for adsorption of iron ions from potable water

Abu-Alhassan Abd-Elshafi<sup>1,\*</sup>, Amer A. Amer<sup>2</sup>, A. El-Shater<sup>3</sup>, Mahmoud Elrouby<sup>2,4</sup>

<sup>1</sup> Sohag Drinking Water & Sanitation Company., Sohag, Egypt

<sup>2</sup> Chemistry Department, Faculty of Science, Sohag University, Sohag, Egypt, 82524

<sup>3</sup> Geology Department, Faculty of Science, Sohag University, Sohag, Egypt, 82524

<sup>4</sup> King Salman International University, Faculty of Science, Ras Sudr, 46612, Sinai, Egypt

Received: 26 Feb. 2022, Revised: 9 Mar. 2022, Accepted: 22 Mar. 2022.

Published online: 1 May 2022

**Abstract:** Natural clays have played a significant role in the adsorption of water pollutants in recent decades. Clays and their modified forms have been examined extensively for the adsorption of both inorganic and organic pollutants by many researchers. The utilization of sodium montmorillonite and various organically modified forms for ferrous ion adsorption was investigated in this study. In our investigation, adsorption isotherms show the physisorption type of Fe(II) adsorption on sodium montmorillonite while The adsorption of iron ions on the modified montmorillonite with 3-mercaptopropyl trimethoxysilane exhibits mixed physisorption and chemisorption characters. The kinetics of adsorption is best represented by pseudo-second-order for all three clays' samples in our investigation, and the adsorption exhibits mixed Boyd film and intraparticle diffusion processes.

**Keywords:** Potable water - ferrous ions – adsorption - Egyptian montmorillonite clay - mercaptopropyl trimethoxysilane modified.

## 1 Introduction

The need for potable water increases with the increasing population in Egypt. People who live in rural and nomadic areas depend mainly on groundwater. Also, Urban expansion plans outside the Nile Valley pose a challenge for us to solve the chronic problems of groundwater. The groundwater contains many undesirable metallic cations that affect the quality of potable water according to Egyptian standards. The cations of widest occurrence in these areas are iron and manganese cations. The problem of occurrence of iron and manganese was the direct reason for neglecting many wells because of the exceeding of their concentrations the values set out in the Minister of Health's decision 2007. Iron is found in deep wells where water has been in contact with rocks for a long time. High levels of iron can discolor the water [1]. Staining and deposition of iron ions in the water distribution system lead to an increase in the color intensity and turbidity [2]. Therefore, the rehabilitation of these wells has become very important in order to avoid the many health problems that these two components cause in the long run. There are many techniques in the adsorption methods for the remediation of iron. These techniques depend on the material used, e.g. activated carbon [3], metal

oxide [4], clays minerals [1], organo-clays [5]. Clays and their modified forms have great attention due to their plenty, cheapness, high efficiency, and being environmentally benign [6].

Smectite-rich clay deposits of different ages occur widely within the Nile valley, delta, and the Western and Eastern Deserts of Egypt [7]. The Egyptian Sohag area has the Pliocene clay deposit composed mainly of smectites in association with a low quantity of kaolinite minerals [8] and has a moderate to high swelling potential [9]. Clay minerals usually have a large surface area, may reach up to 800 m<sup>2</sup>/g [10], and have an electrical charge on their surface which results in the electrostatic attraction of inorganic and organic cations. This charge is caused by isomorphic substitution within the crystal structure, defects, and broken edges of clay minerals [11].

Montmorillonites are the most common clay minerals in the smectite group. It is a 2:1 type clay, which consists of two tetrahedral sheets of central Si atom linked by one central octahedral sheet of central Al atom [12], the three sheets together form a layer. The clay mineral consists of layers stacked over each other called aligned lamellae [13].

\* Corresponding author E-mail: [aboalhassan20082000@gmail.com](mailto:aboalhassan20082000@gmail.com)

This gives montmorillonite high degrees of swelling, potential, and hydrophilicity (Zuzana Navratilova and Martin Mucha, 2015) and, in turn, the ability for modification [6]. The modification of montmorillonite to increase its adsorption ability had specific attention, especially for removing heavy metals from potable water and wastewater [15]. There are many types of modification, including acid washing [16], thermal treatment [17], intercalation with organic compound [18], and grafting a ligand (ligand functionalization) on the surface of the clay through a reaction between the silanol groups (-Si-OH) and an organic alkoxy silane compound supporting the ligand [19].

Intercalation involves replacing exchangeable cations ( $\text{Na}^+$  or  $\text{Ca}^{2+}$ ) in montmorillonite with cationic or anionic long-chain organic compounds (such as quaternary alkylammonium or dodecyl sulfate) to change its surface properties from hydrophilic to hydrophobic and then increasing the intermediate distance between lamellae to increase their affinity for organic contaminants [20] or hosting or grafting a chelating agent [21]. The adsorption performance of the organoclays would be also improved due to their high charge density and special functional groups in the interlayer [22]. Ca-Montmorillonite modified with organic chains attached to chelating agent was used for removing heavy metals from water by either batch or column methods [21].

Many works had concerned on ligand functionalization of mesoporous silica as SBA-15 [23], MCM-41 [24], or montmorillonite [25]. It can be concluded that the method depends on using a silica source such as tetraethoxysilane (TEOS) with/ without clay and mixed with a surfactant such as hexadecyltrimethylammonium bromide (HDTMA-Br) dissolved in alcohol for an appropriate time. After that, the surfactant is removed by either calcination at above 350 °C or releasing the surfactant by refluxing in a nonpolar solvent. The mesoporous silica is then refluxed in a dry organic solvent as toluene or xylene with ligand attached to organ alkoxy silane such as (-Cl, -SH, and -NH<sub>2</sub>) propyl trimethoxysilane (silylation) at an appropriate temperature. The collected new hybrid material is then dried at a moderate temperature [23-25].

This research is devoted to investigating the uptake of iron (II) from water, using available Egyptian clay and its modified form. This can be achieved by employing Na-montmorillonite (MMT-Na), its modified form by sodium dodecyl sulfate (MMT-SDS), and the grafting form of montmorillonite by 3-mercaptopropyl trimethoxysilane (MMT-MPTMS) clay.

## 2 Materials and methods

### Clay preparation

Ca-montmorillonite clay was handled by prof. El-Shater [26]. Na-montmorillonite where 20 g of this clay was dispersed in 500 mL 1 N NaCl for 12 h, then supernatant decanted. After that, another 500 mL of 1 N NaCl was

added to the residue and stirred for 12 h to make sure the cation exchange interacted. The supernatant was decanted again and washed with bi-distilled water followed by centrifugation several times till trace chloride remained. The final wet precipitate was dried in an oven at 70-80 °C. The dried clay (denoted as MMT-Na) was then crushed to a fine powder using mortar and pestle and stored at room temperature in a closed dry glass tube for further use.

MMT-SDS was prepared by dispersing MMT-Na in an appropriate amount of bi-distilled water for 30 min. A weight of sodium dodecyl sulfate equivalent to twice of CEC of MMT-Na is added to the dispersion and stirred at room temperature for 6 hours. The resulting modified clay was separated by centrifugation at 2500 rpm for 30 min then dried at 70 °C.

MMT-MPTMS is prepared by dispersing 5 g of MMT-SDS in 50 mL of Toluene for 30 min in a closed conical flask, then adding 5 mL of 3 mercaptopropyl trimethoxysilane (MPTMS). The dispersion is stirred for 6 hours at room temperature, the resulting hydrophobic clay composite was separated by centrifugation at 2500 rpm for 30 min. Then, the composite is washed with acetone to remove the residual and adsorbed toluene. The supernatant acetone is removed by centrifugation at 2500 rpm for 30 min and decanted. The MMT-MPTMS is then dried at 70 °C. The process of washing MMT-MPTMS by acetone returning it to the hydrophilic character for the modified clay to be suitable for uptaking the iron(II) from an aqueous medium. The whole process is described in figure 1.

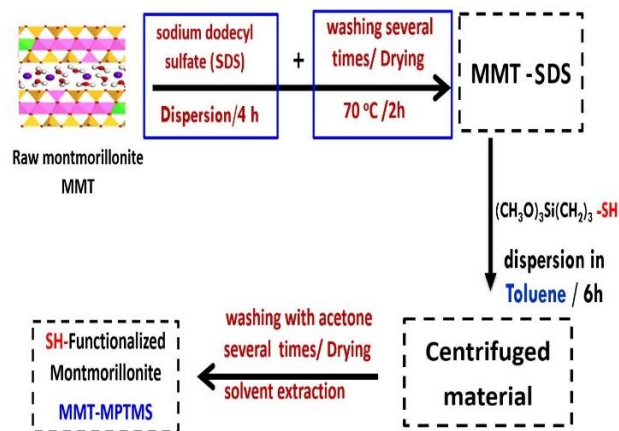


Fig.1: Preparation of MMT-MPTMS

### Instrumentation

The X-ray diffractometer (Burker D8 Advance) with  $K_{\alpha}$  copper radiation ( $\lambda=1.542 \text{ \AA}$ ) was used, with monitoring the diffraction  $2\theta$  angles, 0.023 step size from 4 to 70°, the voltage =30 kV and current=30 mA were used. Infrared spectroscopy of the ATR-FT-IR spectrometer from Burker scans from 4000-400  $\text{cm}^{-1}$  was used. Centrifuge model K241 from Centurion Scientific with rotor type BRK5508L was used for separation of the prepared clays from their

solvents, and separation of adsorbent clay from the analyte solution. pH meter model 3510 from JANEWAY was used to Adjust the pH. Magnetic Stirrer model Nemko from VELD. SCIENTIFICA was used for adsorption mixture stirring at 150 rpm. The distilled water of conductivity  $< 2 \mu\text{S}/\text{cm}$  was produced from water distillation model AC-18 from J.P SELECTA.

A spectrophotometer of model CECIL 3021 was used for spectrophotometric determination of residual ferrous ions in the supernatant. The nonlinear fitting of the adsorption and kinetic models was performed by OriginLab 2019b software using of Levenberg-Marquardt iteration algorithm.

## Materials

Ferrous sulfate ( $\text{FeSO}_4 \cdot 7\text{H}_2\text{O}$ ), ammonium acetate, acetic acid, hydroxylamine hydrochloride, concentrated hydrochloric acid, sodium hydroxide, sodium chloride, ethanol, methylene blue dye, ethylenediamine, anhydrous copper sulfate, TRIS, sodium thiosulfate pentahydrate, potassium dichromate, potassium iodide, potassium hydrogen phthalate, toluene, sodium dodecyl sulfate (SDS) and 3-mercaptopropyle trimethoxysilane (MPTMS) are of analytical grade and used without further purification.

## Procedure

The batch adsorption system was six 100 mL beakers in each 25 mL of ferrous ion and 0.025 g (1 g/L) of sodium or organo-montmorillonite clay. After appreciating contact time, 10 mL from each beaker was then centrifuged at 3000 rpm for 30 min. 5 mL of supernatant was analyzed to determine the residual dissolved iron according to method 3500 Fe-B [27].

## 3 Results and Discussion

### X-ray diffraction

From Figure 2, it can be noted that an increase in d spacing between montmorillonite sheets with modification by SDS, since the long aliphatic chain helps in opening the lamellae. While no increase in d spacing after the addition of MPTMS was observed. It can be concluded that during the solvent extraction process of SDS the MPTMS is grafted simultaneously, making the opening of lamellae is still not changed.

### Infrared spectroscopy

From Figure 3, it appears that the IR Spectra of MMT-Na form has the characteristic vibrations of Montmorillonite. The two stretching vibrations at 3694 and

3619  $\text{cm}^{-1}$  of Si-OH and H-O-H appeared. Moreover, the bending of H-O-H of adsorbed water at 1637  $\text{cm}^{-1}$ , and the vibration of Si-O-Si at 993  $\text{cm}^{-1}$  were observed [28].

The spectra of MMT-SDS exhibit additional peaks, at 2919, 2851  $\text{cm}^{-1}$  characteristic for the stretching of methyl and methylene of the aliphatic chain. At 1384, 1216  $\text{cm}^{-1}$  the characteristic peaks of (O=S=O) of the sulfate group has been observed [29]. The spectra of MMT-MPTMS exhibit low intensity for ( $\text{CH}_2$ -, the propyl group in MPTMS appears at 2968  $\text{cm}^{-1}$ . A strong peak at 1737  $\text{cm}^{-1}$  has been observed, due to the traces of acetone solvent.

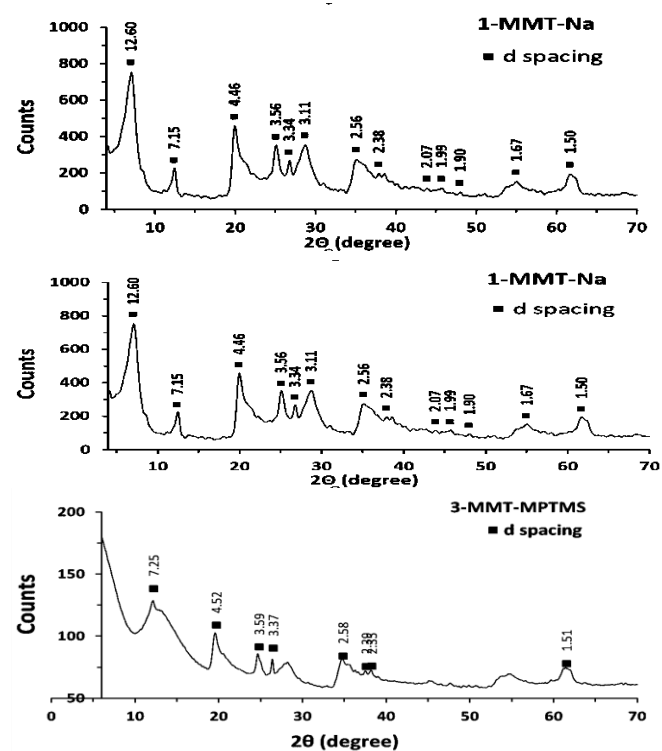


Fig. 2: XRD pattern for the MMT-Na, MMT-SDS, and MMT-MPTMS clays, the step scan  $2\theta=0.023$ .

### specific surface area (SSA)

The specific surface area (SSA) of Na-MMT has been determined to be 68.7  $\text{m}^2/\text{g}$  according to the Sears method [30]. In this method, a sample containing 0.50 grams of silica is acidified with dilute hydrochloric acid to a pH of 3 to 3.5. 10 grams of sodium chloride was added to this solution, and the volume is completed to 50 ml with bi-distilled water. The temperature is adjusted to  $25 \pm 0.5$   $^{\circ}\text{C}$  via an ultra-thermostat. The resultant solution was titrated with standard 0.10 N sodium hydroxide. The base is added to the acidified solution to a pH 4.0 and added further until the pH rises to a steady value of 9.00. The titer is the

volume required to raise the pH from 4.0 to 9.00. 0.01 N NaOH. the SSA is calculated from the empirical formula;

$$S=32 V-25 \quad (1)$$

where  $S$  is Specific surface area and  $V$  is titer volume. The specific surface area of MMT-Na was determined using the methylene blue method to be  $700 \text{ m}^2/\text{g}$  [31]. The difference in measuring the surface area between Sears and methylene methods is that Sears's methods measure only the external silanol-containing surface, while the methylene blue measures both internal and external surfaces.

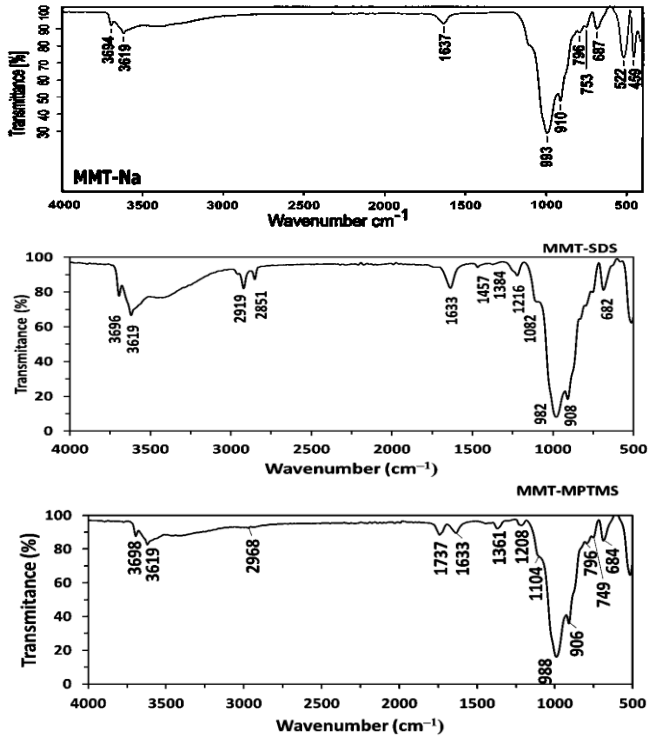


Fig.3: The FTIR for MMT-Na, MMT-SDS, and MMT-MPTMS clays

### cation exchange capacity

The cation exchange capacity of Na-MMT was determined to be about  $86.7 \text{ mmol}/100\text{g}$  according to the Meier-Khars method [32], in which Cu (II) Diene complex adsorbed stoichiometrically on the surface of clay as in the cation exchange mechanism.

### The parameter affects the Adsorption of ferrous ion

#### • Effect of pH

In all three clay types, the pH value is a critical parameter for the adsorption process. Since in low pH values, the adsorption decreases greatly due to competition of  $\text{H}^+$  located in the adsorption sites of the clay. While on a larger pH value ( $\text{pH} > 5.5$ ), the ferrous ions will precipitate as ferrous hydroxide so the  $\text{pH} = 5$  was the best pH used for adsorption. The pH was adjusted using  $0.01 \text{ N H}_2\text{SO}_4$  or

#### • Effect of contact time

From Figure 4, it can be noted that the adsorption on MMT-Na is very fast and reaches the maximum value at a very short time and becomes approximately constant with time. This is due to the pure physisorption process. While the adsorption on MMT-SDS and MMT-MPTMS is still increasing with time due to some slow addition reactions after the addition of modifiers.

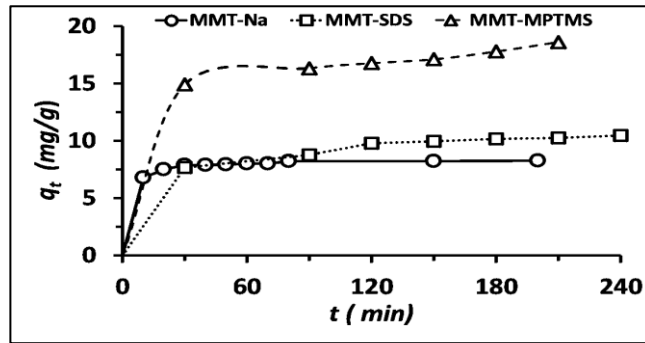


Fig. 4: Effect of contact time on adsorption of  $\text{Fe}^{2+}$  on clays MMT-Na ( $C_0 = 10 \text{ mg/L}$  &  $m = 0.025 \text{ g}$ ), MMT-SDS ( $C_0 = 20 \text{ mg/L}$  &  $m = 0.02 \text{ g}$ ), and MMT-MPTMS ( $C_0 = 20 \text{ mg/L}$  &  $m = 0.015 \text{ g}$ ),  $V = 0.025 \text{ L}$ ,  $\text{pH} = 5$  and  $T = 298 \text{ K}$ .

### Adsorption isotherms

There are many adsorption isotherms types, the adsorption according to Langmuir, Freundlich, Dubinin Radushkevich (D-R) isotherms have been studied. The measured signal for these isotherm models is the amount of adsorbed iron (II) at equilibrium ( $q_e \text{ mg/g}$ ), which can be calculated from the relation:

$$q_e = \frac{(C_0 - C_e)V}{m} \quad (2)$$

### Langmuir isotherm

This adsorption isotherm model is describing saturated monolayer adsorption on the adsorbent surface and postulates that the energy of adsorption is constant and no transmigration of adsorbate molecules [33]. Langmuir adsorption isotherm is described by the following equation:

$$q_e = \frac{q_m K_L C_e}{1 + K_L C_e} \quad (3)$$

where  $q_m \text{ (mg/g)}$  is the maximum adsorption capacity,  $K_L \text{ (L/mg)}$  is a constant that relates to the heat of adsorption [34]. The Langmuir relation can be linearized in the most common form as follows:

$$\frac{C_e}{q_e} = \frac{1}{K_L q_m} + \frac{1}{q_m} C_e \quad (4)$$

As can be seen from Table (1) and Figure (5), the linear and nonlinear Langmuir isotherm is the best-fitted isotherm for

MMT-Na MMT-SDS and MMT-MPTMS. This is because of the high surface areas of the pristine clay MMT-Na and high interaction forces between adsorption sites and  $\text{Fe}^{2+}$ . The values of  $q_m$  and  $K_L$  are quite close in the linear and nonlinear fitting of Langmuir isotherm which means a good agreement between the two fitting equations. Separation factor [35]. It is found that obtained values in all ranges are favorable. The separation factor can be calculated from the following equation:

$$R_L = \frac{1}{1 + K_L C_0} \quad (5)$$

The maximum adsorption capacity  $q_m$  (mg/g) increases in the order of MMT-Na < MMT-SDS < MMT-MPTMS. This is because SDS increases the d spacing between lamellae. While in MMT-MPTMS, two factors affect adsorption. The first factor is the d spacing opening “the same as in MMT-SDS (Fig. 2)”. The second factor is the interaction between the soft ligand thiol group and the soft  $\text{Fe}^{2+}$  according to the Hard and Soft Acids and Bases (HSAB) principle [36]. This makes adding some chemical adsorption.

### Freundlich isotherm

This Freundlich model [37] can be applied to the adsorption on heterogeneous surfaces with molecule-molecule

interactions. This model assumes that as the adsorbate concentration increases, the concentration of adsorbate on the adsorbent surface also increases without limitation [38].

The equation for the Freundlich model is given as follows;

$$q_e = K_F C_e^{\frac{1}{n}} \quad (6)$$

and the linearized form is:

$$\log q_e = \log K_F + \frac{1}{n} \log C_e \quad (7)$$

where  $K_F$  is the Freundlich constant related to the adsorption capacity,  $1/n$  is the heterogeneity factor which is related to the intensity of the adsorption [39].

From data collected in Table (1), it is observed that Freundlich isotherm has lower linearity in all clays. This indicates that in all clays the mono surface layer adsorption is favorable. The Freundlich factor  $1/n$  is <1 in all clays. This is another argument that elucidates that adsorption is favorable but without effective heterogeneity.

The  $K_F$  constant increases as  $q_m$  increases of the order MMT-Na < MMT-SDS < MMT-MPTMS. The data in linear and nonlinear fittings of Freundlich isotherm are close, this confirms the validity of the results.

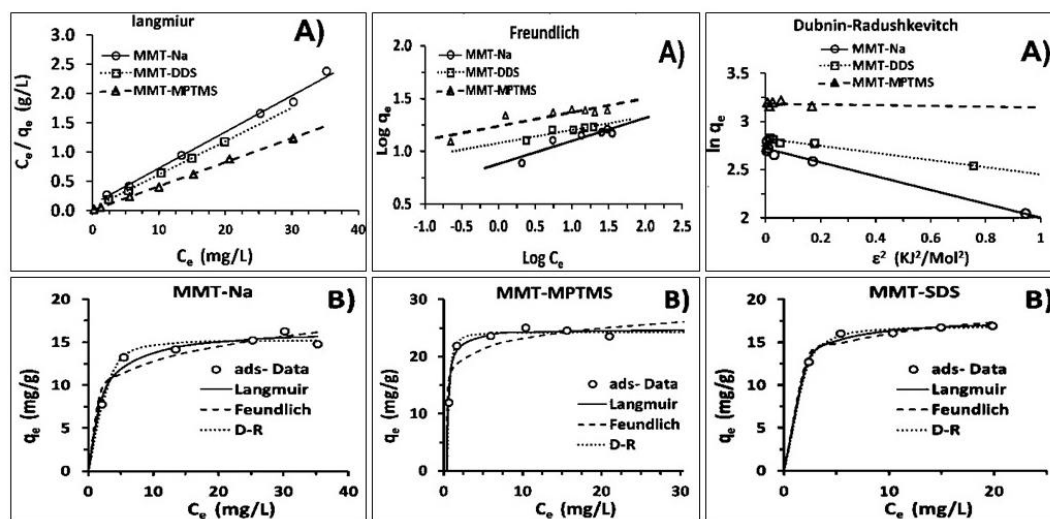


**Fig. 5:** A) linear B) Nonlinear fitting of Langmuir, Freundlich and Dubinin-Radushkevich isotherms for the adsorption of Fe (II) on clays MMT-Na ( $C_0 = 10\text{-}60$  mg/L and  $m=0.025$  g), MMT-SDS ( $C_0 = 10\text{-}60$  mg/L and  $m=0.015$  g), MMT-MPTMS ( $C_0 = 5\text{-}40$  mg/L and  $m=0.015$  g),  $T = 298$  K, contact time = 150 min, pH = 5 and  $V = 0.025$  L.

### Dubinin–Radushkevich Isotherm (DR)

This model involves both mono- and multi-layer adsorption [39]. The model was usually applied to distinguish the physical and chemical adsorption of metal ions with its mean free energy [40]. When the value of adsorption energy ( $E_D$ ) is < 8 kJ/mol, the adsorption process can be considered

as physisorption. While if the value of  $E_D$  is located in the range of 8 - 16 kJ/mol, it will be a chemisorption process [41]. The model equation is given as the following:

$$q_e = q_s e^{-K_D \varepsilon^2} \quad (8)$$

where  $q_s$  (mg/g) is the DR monolayer capacity constant,  $K_D$  ( $\text{Mol}^2/\text{KJ}^2$ ) is the DR constant related to adsorption energy,

and  $\varepsilon$  ( $KJ^2/Mol^2$ ) is the Polanyi's potential which is related to the free energy of adsorption [12]. The linearized form can be represented as follows:

$$\ln q_e = \ln q_s - K_D \varepsilon^2 \quad (9)$$

The Polanyi's potential  $\varepsilon$  is given from the following relation:

$$\varepsilon = RT \ln(1 + \frac{1}{C_e}) \quad (10)$$

and the adsorption energy  $E_D$  can be calculated from:

$$E_D = \frac{1}{\sqrt{2K_D}} \quad (11)$$

As can be seen from Table (1) and Figure (5),  $R^2$  of D-R isotherm of the three clays is high for linear and nonlinear fitting, confirming that the Langmuir is the best fitting model. The  $q_s$  constant increases as in the order MMT-Na < MMT-SDS < MMT-MPTMS.

$E_D$  for MMT-Na = 0.834  $KJ/mol$ , which indicates physisorption. This means that the weak Van Der Waals interactions play the main role. The  $E_D$  for MMT-SDS is equal to 1.164  $KJ/mol$ . This value is higher than that of MMT-Na. The value of  $E_D = 3.523$   $KJ/mol$  for MMT-MPTMS is high but lower than 8  $KJ/mol$ . This indicates that the thiol group works as a ligand and interacts with  $Fe^{2+}$  through chemical bonding

**Table 1:** linear and nonlinear fitting of Langmuir, Freundlich, and Dubinin-Radushkevich isotherms for the adsorption of Fe (II) on studied clays.

### 1-Linear fitting

clay	Langmuir				Freundlich			Dubinin-Radushkevich (298 <sup>0</sup> K)			
	$q_m$ mg/g	$K_L$ L/mg	$R^2$	$R_L$	$\frac{1}{n}$	$K_F$	$R^2$	$q_s$ mg/g	$K_D$ Mol <sup>2</sup> /KJ <sup>2</sup>	$E_D$ KJ/Mol	$R^2$
MMT-Na	16.17	0.597	0.995	0.032-0.144	0.258	7.151	0.826	15.2	0.719	0.834	0.993
MMT-SDS	17.57	1.284	0.999	0.025-0.72	0.142	11.68	0.832	16.68	0.370	1.163	0.981
MMT-MPTMS	24.42	23.476	0.999	0.001-0.008	0.131	17.26	0.756	24.2	3.527	3.523	0.993

### 2- Nonlinear fitting

clay	Langmuir			Freundlich			Dubinin-Radushkevich (298 <sup>0</sup> K)			
	$q_m$ mg/g	$K_L$ L/mg	$R^2$	$\frac{1}{n}$	$K_F$	$R^2$	$q_s$ mg/g	$K_D$ Mol <sup>2</sup> /KJ <sup>2</sup>	$E_D$ KJ/Mol	$R^2$
MMT-Na	16.56	0.501	0.995	0.186	8.330	0.954	15.24	0.731	0.827	0.990
MMT-SDS	17.75	1.152	0.940	0.117	12.193	0.820	16.84	0.369	1.164	0.977
MMT-MPTMS	27.79	4.43	0.980	0.105	18.28	0.727	24.22	0.041	3.511	0.987

**Table 2:** Langmuir and Freundlich coefficients in previous studies on adsorption of Fe (II) or Fe (III).

adsorbate	Adsorbent	Langmuir			Freundlich			Reference
		$q_m$ (mg/g)	$K_L$ (L/mg)	$R^2$	$n$	$K_F$	$R^2$	
Fe (II)	limestone	0.03	1	0.84	2.7	0.03	0.83	[42]
Fe (II)	natural shell	4.91	4.39	0.986	7.3	3.93	0.985	[43]
Fe (II)	CS:PEG 1:1 *	71.4	0.359	0.787	15.6	0.05	0.832	[44]
Fe (II)	CS:PEG 2:1	90.9	0.333	0.682	16.4	0.04	0.703	[44]
Fe (III)	Na-MMT	28.9	0.085	0.990	2.5	5.2	0.97	[45]
Fe (III)	Activated Na-MMT	30	0.116	0.990	3.33	6.4	0.96	[45]
Fe (III)	kaolinite	11.2	0.035	0.990	2.5	1.3	0.98	[45]
Fe (III)	Activated kaolinite	12.1	0.043	0.990	2.5	1.7	0.97	[45]
Fe (II)	MMT-Na	16.17	0.597	0.995	3.88	7.151	0.826	This work
Fe (II)	MMT-SDS	17.57	1.284	0.999	7.04	11.68	0.832	This work
Fe (II)	MMT-MPTMS	24.42	23.476	0.999	7.63	17.26	0.756	This work

\*microporous chitosan/polyethylene glycol blend membrane

### Adsorption Kinetic Models

The linear and nonlinear fitting models of the pseudo-first-order (PFO) and the pseudo-second-order (PSO)

have been studied. The linear and nonlinear Elovich model, Boyd, weber, and Morris intraparticle diffusion Models have been also discussed.

### Pseudo first order and pseudo-second-order models

The Pseudo first-order model has been given by Lagergren relation as follows [46]:

$$q_t = q_e(1 - e^{-K_1 t}) \quad (12)$$

where  $q_t$  is the amount of adsorbate per gram of adsorbent at time  $t$ . It can be calculated from the following equation:

$$q_t = \frac{(C_0 - C_t)V}{m} \quad (13)$$

The linearized form of the PFO model is as follows.

$$\ln(q_e - q_t) = \ln q_e - K_1 t \quad (14)$$

While the PSO model applied to adsorption from liquids had been given by Ho et al. [47], its nonlinear equation its nonlinear equation is as follow:

$$q_t = \frac{q_e^2 K_2 t}{q_e K_2 t + 1} \quad (15)$$

The linearized form [48] of this equation is:

$$\frac{t}{q_t} = \frac{1}{K_2 q_e^2} + \frac{t}{q_e} \quad (16)$$

The process of linearization can cause inaccurate determination of the fitting parameters. So the nonlinear fitting can provide additional confirmation of the best fitting model [49]. It is good to compare the PFO fitting parameter from the equations (12), (14) and the PSO fitting parameter from the equations (15), (16) to see the best model describing the kinetics of the adsorption. From Fig. 6 and Table 3, it can be noticed that the best fitting kinetic model is PSO for adsorption of  $\text{Fe}^{2+}$  on MMT-Na, MMT-SDS, and MMT-MPTMS. From the linear and nonlinear fittings, it can be seen that the calculated values of  $q_e$  (mg/g) are close to the corresponding experimental. This confirms that the MMT-MPTMS exhibit electron sharing between the thiol group and  $\text{Fe}^{2+}$  ions.

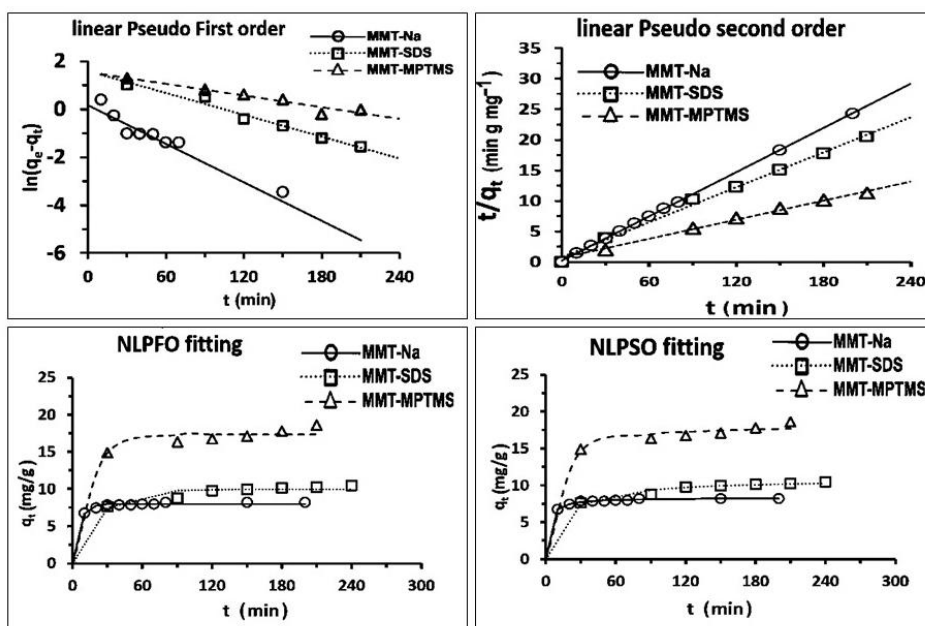


**Fig. 6:** Linear and nonlinear, fitting of PFO and PSO models of adsorption of  $\text{Fe}^{2+}$  on clays MMT-Na ( $C_0 = 10 \text{ mg/L}$  &  $m = 0.025 \text{ g}$ ), MMT-SDS ( $C_0 = 20 \text{ mg/L}$  &  $m = 0.02 \text{ g}$ ), and MMT-MPTMS ( $C_0 = 20 \text{ mg/L}$  &  $m = 0.015 \text{ g}$ ),  $V = 0.025 \text{ L}$ ,  $\text{pH} = 5$  and  $T = 298 \text{ K}$ .

### Elovich model

The Elovich equation can be applied to chemical adsorption kinetics [50]. The Elovich equation is often valid for systems in which the adsorbing surface is heterogeneous [51]. The equation of Elovich is as follows.

$$q_t = \frac{1}{b} \ln(t + t_0) - \frac{1}{b} \ln(t_0) \quad (17)$$

where  $t_0 = 1/ab$ , If  $t \gg t_0$ , the equation can be simplified to the linearized form as follows.

$$q_t = \frac{1}{b} \ln(t) + \frac{1}{b} \ln(ab) \quad (18)$$

From Figure (7) and Table (6), we can see that the Elovich model for adsorption in MMT- SDS and MMT-MPTMS have a higher  $R^2$  value than the pristine MMT-Na. This may be attributed to the iron species combined by physical and chemical adsorption on the surface of the modified form.

Good agreement between linear and nonlinear fitting is observed.

The  $t_0$  (min) as calculated from the model has a very small value for all clays, this indicates that the adsorption process starts immediately as any clay and  $\text{Fe}^{2+}$  solution is mixed.

**Table 3:** Linear and nonlinear, fitting of PFO and PSO models of adsorption of  $\text{Fe}^{2+}$  on clays MMT-Na ( $C_0 = 10 \text{ mg/L}$  &  $m = 0.025 \text{ g}$ ), MMT-SDS ( $C_0 = 20 \text{ mg/L}$  &  $m = 0.02 \text{ g}$ ), and MMT-MPTMS ( $C_0 = 20 \text{ mg/L}$  &  $m = 0.015 \text{ g}$ ),  $V = 0.025 \text{ L}$ ,  $\text{pH} = 5$  and  $T = 298 \text{ K}$ .

clay	Fitting model	$q_e$ (exp) mg/g	Pseudo First Order			Pseudo Second Order		
			$K_1$ min <sup>-1</sup>	$q_e$ (Calc.) mg/g	$R^2$	$K_2$ g mg <sup>-1</sup> min <sup>-1</sup>	$q_e$ (Calc.) mg/g	$R^2$
MMT-NA	Linear	8.24	0.027	1.18	0.850	0.0516	8.33	1.000
	Nonlinear		0.176	8.00	0.995	0.0522	8.33	0.999
MMT-SDS	Linear	10.45	0.015	4.90	0.973	0.0050	11.14	0.998
	Nonlinear		0.046	9.95	0.983	0.0067	10.83	0.994
MMT-MPTMS	Linear	18.6	0.014	10.36	0.859	0.0037	19.23	0.994
	Nonlinear		0.065	17.33	0.988	0.0072	18.31	0.993

**Table 4:** Linear and nonlinear, fitting of Elovich model of adsorption of  $\text{Fe}^{2+}$  on clays MMT-Na ( $C_0 = 10 \text{ mg/L}$  &  $m = 0.025 \text{ g}$ ), MMT-SDS ( $C_0 = 20 \text{ mg/L}$  &  $m = 0.02 \text{ g}$ ), and MMT-MPTMS ( $C_0 = 20 \text{ mg/L}$  &  $m = 0.015 \text{ g}$ ),  $V = 0.025 \text{ L}$ ,  $\text{pH} = 5$  and  $T = 298 \text{ K}$ .

Clay	$t_0$ (min)		$a$ (mg g <sup>-1</sup> min <sup>-1</sup> )		$b$ (g/mg)		$R^2$	
	Linear	Nonlinear	Linear	Nonlinear	Linear	Nonlinear	Linear	Nonlinear
MMT-Na	0.00	0.00	311221.8	313259.4	2.215	2.216	0.824	0.824
MMT-SDS	0.13	0.13	10.69	10.55	0.716	0.133	0.964	0.997
MMT-MPTMS	0.01	0.01	293.4	293.0	0.583	0.583	0.917	0.997

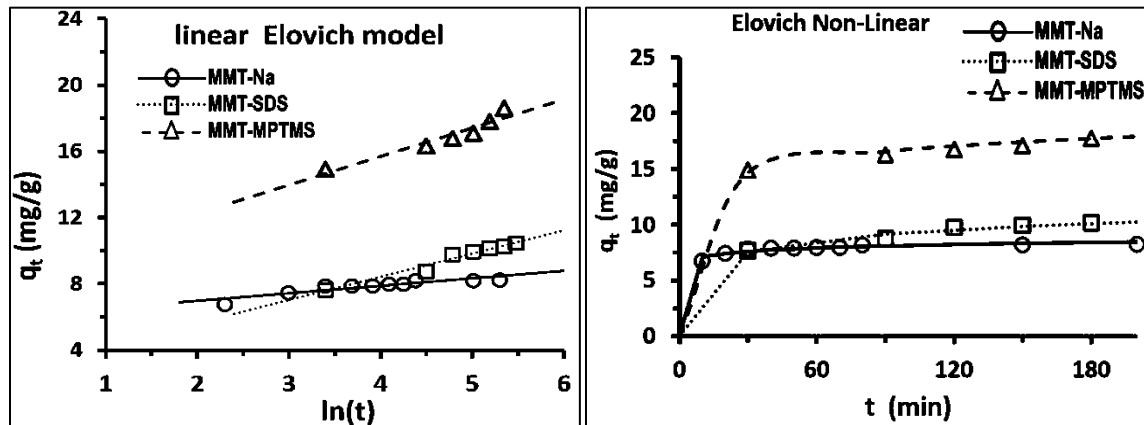


**Fig. 7:** Linear and nonlinear, fitting of Elovich model of adsorption of  $\text{Fe}^{2+}$  on clays MMT-Na ( $C_0 = 10 \text{ mg/L}$  &  $m = 0.025 \text{ g}$ ), MMT-SDS ( $C_0 = 20 \text{ mg/L}$  &  $m = 0.02 \text{ g}$ ), and MMT-MPTMS ( $C_0 = 20 \text{ mg/L}$  &  $m = 0.015 \text{ g}$ ),  $V = 0.025 \text{ L}$ ,  $\text{pH} = 5$  and  $T = 298 \text{ K}$ .

### Adsorption mechanism

Many mechanisms can be used to determine the rate-limiting step of the transition of  $\text{Fe}^{2+}$  adsorbate to the unmodified and modified montmorillonites adsorbents. Boyd et al suggested two different mechanism models; diffusion through abounding liquid film (film diffusion) and diffusion in and through adsorbent particles (intraparticle diffusion) [52]. While Weber and Morris had another mechanism model of intraparticle diffusion [53]. The overall adsorption process can be controlled by one or more

of these steps [54].

### Boyd liquid film diffusion model

This model can be described by the following equation;

$$\ln(1-F) = -kt \quad (19)$$

where  $F$  is the fractional attainment of equilibrium =  $q/q_e$ ,  $k$  is constant related to liquid film diffusion coefficient [52]. Equation (19) shows that the fitting line should pass through the origin. From Table 5 and Figure 8, all intercepts are

relatively small with moderate linearity ( $R^2 = 0.85-0.97$ ). This means that there is a contribution of the boundary liquid film diffusion of the whole adsorption process on all clays. This indicates that this step is quite slow but not completely the rate-determining step.

#### Boyd intraparticle diffusion model

This model describes the diffusion in and through the particles of the adsorbent [52]. The model can be described mathematically by the following equation:

$$F = 1 - \frac{6}{\pi^2} \sum_{n=1}^{\infty} \frac{1}{n^2} e^{-n^2 Bt} \quad (20)$$

where  $B$  is the rate coefficient related to the diffusion coefficient [52],  $n$  is an integer number,  $Bt$  can be converted to a function of  $F$  when applying the Fourier transform [55] to equation (20) as in the following:

$$0 \leq F \leq 0.85: \quad Bt = 2\pi - \frac{\pi^2 F}{3} - 2\pi \left(1 - \frac{\pi F}{3}\right)^{\frac{1}{2}} \quad (21)$$

$$0.86 \leq F \leq 1: \quad Bt = -0.498 - \ln(1 - F) \quad (22)$$

A relation between  $t$  (min) on the x-axis and  $Bt$  on the y-axis should be linear and the fitting line passes through the origin.

From Table 5 and Figure 8, it is observed that all intercepts

**Table 5:** linear fitting of liquid film diffusion Boyd and intraparticle diffusion Boyd and Weber & Morris models of adsorption of  $\text{Fe}^{2+}$  on clays MMT-Na ( $C_0 = 10 \text{ mg/L}$  &  $m = 0.025 \text{ g}$ ), MMT-SDS ( $C_0 = 20 \text{ mg/L}$  &  $m = 0.02 \text{ g}$ ), and MMT-MPTMS ( $C_0 = 20 \text{ mg/L}$  &  $m = 0.015 \text{ g}$ ),  $V = 0.025 \text{ L}$ ,  $\text{pH} = 5$  and  $T = 298 \text{ K}$ .

	Boyd film diffusion model			Intraparticle diffusion model					
				Boyd Model			Weber & Morris Model		
	$k(\text{min}^{-1})$	intercept	$R^2$	slope	intercept	$R^2$	$k_p(\text{mg g}^{-1} \text{min}^{-1/2})$	$C(\text{mg/g})$	$R^2$
MMT-Na	0.027	-1.947	0.85	0.027	1.451	0.850	0.205	6.430	0.808
MMT-SDS	0.015	-0.758	0.973	0.015	0.278	0.973	0.624	2.011	0.851
MMT-MPTMS	0.009	-1.273	0.948	0.009	0.784	0.947	0.385	12.66	0.969

## 4 Conclusion

MMT-Na clay which is separated and purified locally has high cation exchange capacity which makes it with good adsorption capacity, while modification with long-chain anionic surfactant SDS enhances slightly the maximum adsorption capacity as we explained by Langmuir isotherm but is not likely to give evidence for increasing widely the chemisorption character and modification with MPTMS gives the best results for the maximum adsorption capacity of  $\text{Fe}^{2+}$ . The adsorption energy calculated from Dubinin-Radushkevich isotherm gives the higher value (3.52 KJ/Mol) among the three clay, this insures the introducing

of the studied relations are not far from the origin point and the linearity is moderate. This indicates that intraparticle diffusion is another step of the adsorption  $\text{Fe}^{2+}$  mechanism, and this step is slow but not only the rate-determining step.

#### Weber and Morris intraparticle diffusion model

This model is of major interest because internal diffusion determines the adsorption rate in most liquid systems [55]. The model [53] is described by the equation as follows:

$$q_t = K_p t^{\frac{1}{2}} + C \quad (23)$$

where  $K_p$  is the intraparticle diffusion rate constant ( $\text{mg g}^{-1} \text{min}^{-1/2}$ ),  $C$  ( $\text{mg/g}$ ) is a constant related to the concentration of adsorbate during the film diffusion step "which is before the intraparticle diffusion step". The closer the value of  $C$  to 0, the more indication that intraparticle is the main rate-determining step. The relation between  $q_t$  and  $t^{1/2}$  may be one linear line or many segment lines, each segment describes a step of adsorption [56]. It is found that for all clays the constant  $C$  is high, this indicates that the intraparticle diffusion is present and best described by the Boyd model rather than Weber & Morris model.

the chemisorption character, although the value is still  $< 8$  KJ/Mol which indicates that both physisorption and chemisorption works as well. The chemisorption character arises from the character interaction between the soft acid  $\text{Fe}^{2+}$  and the soft base -SH group according to Hard-Soft acid and bases principle (HSAB), The best fitting kinetic model linearly and nonlinearly is the PSO for all the three clays. The adsorption proceeded with mixed Boyd film and intraparticle diffusion mechanisms. This makes MMT-MPTMS modified clay with promising properties in its use as an adsorbent for iron from different water sources.

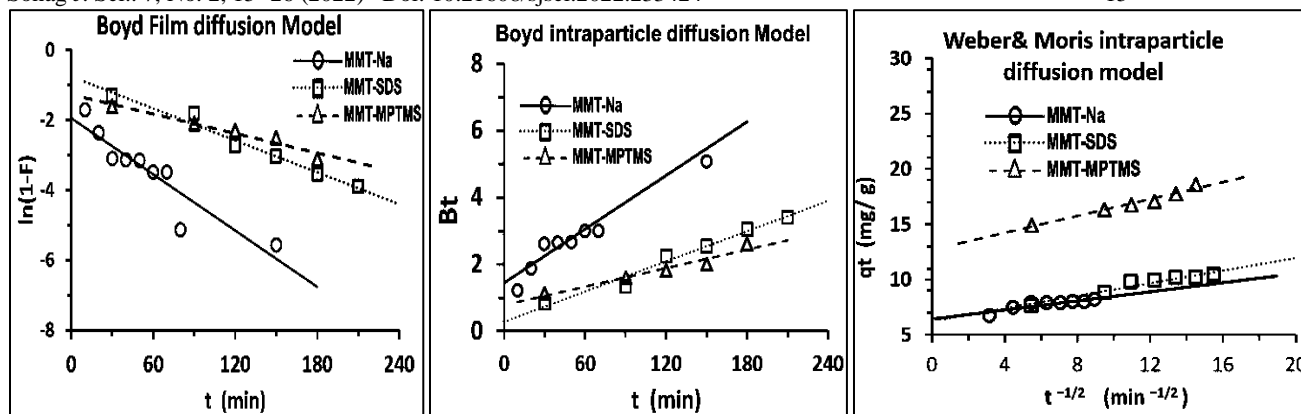


**Fig. 8:** linear fitting of Boyd liquid film diffusion, Boyd intraparticle diffusion and Weber & Morris models of adsorption of  $\text{Fe}^{2+}$  on clays MMT-Na ( $C_0 = 10 \text{ mg/L}$  &  $m = 0.025\text{g}$ ), MMT-SDS ( $C_0 = 20 \text{ mg/L}$  &  $m = 0.02\text{g}$ ), and MMT-MPTMS ( $C_0 = 20 \text{ mg/L}$  &  $m = 0.015\text{g}$ ),  $V = 0.025 \text{ L}$ ,  $\text{pH} = 5$  and  $T = 298 \text{ K}$

## 5 References

- [1] Hassouna, M., Shaban, M., Nassif, M., Removal Of Iron And Manganese Ions From Groundwater Using Kaolin Sub Micro Powder And Its Modified Forms, *International Journal of Bioassays*, 3(7), 137-145, 2014.
- [2] Tekerlekopoulou, A. & Vayenas, D., Simultaneous biological removal of ammonia, iron and manganese from potable water using a trickling filter, *Biochemical Engineering Journal*, 39, 215-220, 2008.
- [3] Akl, M., Yousef, A., AbdElnasser, S., Removal of Iron and Manganese in Water Samples Using Activated Carbon Derived from Local Agro-Residues, *Chemical Engineering & Process Technology*, 4(4), 1-10, 2013.
- [4] Biela, T., & Kucera, T., Efficacy of sorption of materials for nickal iron and manganese removal from water, *Procedia Engineering*, 162, 56-63, 2016.
- [5] Mahadevalah, N., Vijayakumar, B., Hemalatha, K., Jai Prakash, B., Uptake of permanganate from aqueous environment by surfactant modified montmorillonite batch and fixed bed studies, *Indian Academy of Sciences*, 34(7), 1675-1681, 2011.
- [6] Zhu, R., Chena, Q., Zhoua, Q., Xi, Y., Zhua, J., He, H., Adsorbents based on montmorillonite for contaminant removal from water: A review, *Applied Clay Science*, 123, 239-258, 2016.
- [7] Agha, M., Ferrell, R., Hart, G., Abu El Ghar, M., Abdel-Motelib, A., Physical properties and Na-activation of Egyptian bentonitic clays for appraisal of industrial applications, *Applied Clay Science*, 131, 74-83, 2016.
- [8] Refaey, Y., Jansen, B., El-Shater, A., El-Hadad, A., Kalbitz, K., Clay minerals of Pliocene deposits and their potential use for the purification of polluted wastewater in the Sohag area, Egypt, *Geoderma Regional*, 5, 215-225, 215.
- [9] Youssef, A., Mapping the Pliocene Clay Deposits Using Remote Sensing and its Impact on the Urbanization Developments in Egypt: Case Study, East Sohag Area, *Geotech Geol Eng*, 26, 579-591, 2008.
- [10] Michot, L., Villieras, F., Surface Area and Porosity, in *Handbook of Clay Science*, 5B., Elsevier Ltd., 319-332, 2013.
- [11] Schoonheydt, R., Johnston, C., surface and interface chemistry of clay minerals, in *Handbook of clay science*, 1. 1, Elsevier Ltd., 87,88. 2006
- [12] Wypych, F., Satyanarayana, K. *Clay Surfaces: Fundamentals and applications*, Elsevier, 2004.
- [13] Pusch, R., *Bentonite Clay: Environmental Properties and Application*, Boca Raton: CRC Press- Taylor & Francis Group, 2015.
- [14] Navratilova, Z., Mucha, M., Organo-montmorillonites as carbon paste electrode modifiers, *J. Solid State Electrochem.*, 19, 2013-2022, 2015.
- [15] Bhattacharyya, K., Gupta, S., Adsorption of a few heavy metals on natural and modified kaolinite and montmorillonite: A review, *Advances in Colloid and Interface Science*, 140, 114-131, 2008.
- [16] Bhattacharyya, K., Gupta, S., Influence of Acid Activation of Kaolinite and Montmorillonite on Adsorptive Removal of Cd(II) from Water, *Ind. Eng. Chem. Res.*, 46, 3734-3742, 2007.
- [17] Olu-Owolabi, B., Alabi, A., Calcined Biomass-Modified Bentonite Clay for Removal of Aqueous Metal Ions," *Journal of Environmental Chemical Engineering*, 4(1), 1-26, 2016.
- [18] Singla, P., Mehta, R., And Upadhyay, S., Clay Modification by the Use of Organic Cations, *green and Sustainable Chemistry*, 2, 21-25, 2012.

- [19] Aguado, J., Arsuaga, J., Arencibia, A., Lindo, M., Gascón, V., Aqueous heavy metals removal by adsorption on amine-functionalized mesoporous silica, *Journal of Hazardous Materials*, 163, 213-221, 2008.
- [20] Kostelnikova, H., Praus, P., Turicova, M., , Adsorption of phenol and aniline by original and quaternary ammonium salts-modified montmorillonite, *Acta Geodyn. Geomater.*, 5(1), 83-88, 2008.
- [21] Filho, N., Do Carmo, D., Gessner, F., Rosa, A., preparation of a Clay-modified Carbon Paste Electrode Based on 2- Thiazoline-2-thiol-hexadecylammonium sorption for sensitive Determination of Mercury, *Analytical Science*, 21, 1309-1316, 2005.
- [22] Jiang, J., Zeng, Z., Comparison of modified montmorillonite adsorbents. part II: The effects of the type of raw clays and modification conditions on the adsorption performance, *Chemospher*, 53, 53-52, 2003.
- [23] Moorthy, M., Park, S., Selvaraj, M., Ha, C., Cyclic Ligand Functionalized Mesoporous Silica (SBA-15) for Selective Adsorption of  $\text{Co}^{2+}$  Ion from Artificial Seawater, *Journal of Nanoscience and Nanotechnology*, 14(11), 8891-8897, 2014.
- [24] Parambadath, S., Mathew, A., Park, S., Ha, C., Pentane-1,2-dicarboxylic acid functionalized spherical MCM-41: A simple and highly selective heterogeneous ligand for the adsorption of  $\text{Fe}^{3+}$  from aqueous solutions, *Journal of Environmental Chemical Engineering*, 3, 1918-1927, 2015.
- [25] Addy, M., Losey, B., Mohseni, R., Zlotnikov, E., Vasiliev, A., Adsorption of heavy metal ions on mesoporous silica-modified montmorillonite containing a grafted chelate ligand, *Applied Clay Science*, 59-60, 115-120, 2012.
- [26] Elshater, A., Elhaddad, A., Elattaar, A., Abugharbia, M., Soliman, W., Characterisation of the Egyptian Pliocene bentonite from the Sohag region for pharmaceutical use, *Arabian Journal of Geosciences*, 11, 2018.
- [27] Eaton, A., *Standard Methods for the Examination of Water and Wastewater*, Ed., Washington: American Public Health Association(APHA), 23, 1999.
- [28] Helloa, K., Ibrahim, A., Shneine, J., Appaturi, J., Simple method for functionalization of silica with alkyl silane and organic ligands, *South African Journal of Chemical Engineering*, 15, 159-168, 2018.
- [29] Thompson, J., *Infrared Spectroscopy*, Boulevard: Pan Stanford Publishing Pte. Ltd., 2018.
- [30] Sears, G., Determination of Specific Surface Area of Colloidal Silica by Titration with Sodium Hydroxide, *Analytical chemistry*, 28(12), 1983-1983, 1954.
- [31] Hang, P., Brindley, G., Methylene blue absorption by clay Minerals. Determination of surface Areas and cation exchange capacities, *Clays and Clay Minerals*, 18, 203-212, 1970.
- [32] Meier, L., Kahr, G., Determination of the cation exchange capacity (CEC) of clay minerals using the complexes of copper(ii) ion with triethylenetetramine and tetraethylenepentamine, *Clays and Clay Minerals*, 47(3), 386-388, 1999.
- [33] Ananta, S., Saumen, B., Vijay, V., Adsorption Isotherm, Thermodynamic and Kinetic Study of Arsenic (III) on Iron Oxide Coated Granular Activated Charcoal, *International Research Journal of Environment Sciences*, 4(1), 64-77, 2015.
- [34] Yang, F., Sun, S., Chena, X., Chang, Y., Zha,F., Lei, Z., Mg-Al layered double hydroxides modified clay adsorbents for efficient removal of  $\text{Pb}^{2+}$ ,  $\text{Cu}^{2+}$  and  $\text{Ni}^{2+}$  from water, *Applied Clay Science*, 123, 134-140, 2016.
- [35] Weber, T., Charkravorti, R., Pore and solid diffusion models for fixed-bed adsorbents," *AIChE Journal*, 20(2), 228-238, 1974.
- [36] Nascimento, F., Costa, D., Masini, J., Evaluation of thiol-modified vermiculite for removal of  $\text{Hg}(\text{II})$  from aqueous solutions, *applied clay science*, 125, 227-235, 2016.
- [37] Langmuir, I., the adsorption of gases on plane surfaces of glass, mica and platinum., *Journal of the American Chemical Society*, 40(9), 1361-1403, 1918.
- [38] Vijayakumar, G., Tamilarasan, R., Dharmendirakumar, M., Adsorption, Kinetic, Equilibrium and Thermodynamic studies on the removal of basic dye Rhodamine-B from aqueous solution by the use of natural adsorbent perlite, *Journal of Materials and Environmental Science*, 3(1), 157-170, 2012.
- [39] Ayawei, N., Ebelegi, A., Wankasi, D., Department, Modelling and Interpretation of Adsorption Isotherms, *journal of chemistry*, 2017, 2017.
- [40] Dada, A., Olalekan, A., Olatunya, A., DADA, O., Langmuir, Freundlich, Temkin and Dubinin-Radushkevich Isotherms Studies of Equilibrium Sorption of  $\text{Zn}^{2+}$  Unto Phosphoric Acid Modified Rice Husk, *Journal of Applied Chemistry*, 3(1), 38-45, 2012.
- [41] Ibrahim, M., Sani, S., Comparative Isotherms Studies on Adsorptive Removal of Congo Red from Wastewater by Watermelon Rinds and Neem-Tree Leaves, *Open Journal of Physical Chemistry*, 4, 139-146, 2014.

- [42] Akba, N., Abdul Aziz, H., Adlan, M., Iron and Manganese Removal from Groundwater using High Quality Limestone, *Applied Mechanics and Materials*, 802, 460-465, 2015.
- [43] Zhu, C., Wang, S., Hu, K., Wang, W., Cai, A., Chang, W., Li, B., Study on fluoride, iron and manganese removal from aqueous solutions by a novel composite adsorbent, *Advanced Materials Research*, 821-822, 1085-1092, 2013.
- [44] Reiad1, N., Abdel Salam, O., Abadir, E. Harraz, F., Adsorptive removal of iron and manganese ions from aqueous solutions with microporous chitosan/polyethylene glycol blend membrane, *Journal of Environmental Sciences*, 24(8), 1425-1432, 2012.
- [45] Bhattacharyya, K., and Gupta, S., Adsorption of Fe(III) from water by natural and acid activated clays, *Studies on equilibrium isotherm, kinetics and thermodynamics of interactions, Adsorption*, 2006(12), 185-204, 2006.
- [46] Lagergren, S., About the theory of so-called adsorption of soluble substances, *Handlinger*, 24, 1-39, 1898.
- [47] Ho, Y., McKay, G., The kinetics of sorption of divalent metal ions onto sphagnum moss peat, *Water Research*, 34(3), 735-742, 2000.
- [48] El-Khaiary, M., Malash, G., Ho, Y., On the use of linearized pseudo-second-order kinetic equations for modeling adsorption systems, *Desalination*, 257, 93-101, 2010.
- [49] Wang, J., Guoa, X., Adsorption kinetic models: Physical meanings, applications, and solving methods, *Journal of Hazardous Materials*, 390, 2020.
- [50] McIntock, J., The elovich equation in chemisorption kinetics, *Nature*, 216, 1204-1205, 1967.
- [51] Cheung, C., Porter, J., McKay, G., Elovich equation and modified second-order equation for sorption of cadmium ions onto bone char, *Journal of Chemical Technology and Biotechnology*, 75(11), 963-970, 2000.
- [52] Boyd, G., Adamson, A., Myers, L., The Exchange Adsorption of Ions from Aqueous Solutions by Organic Zeolites. Ion-exchange Equilibria, *Journal of the American Chemical Society*, 69(11), 2818-2829, 1947.
- [53] Weber Jr, W., Morris, J., Kinetics of Adsorption on Carbon from Solution, *Journal of the Sanitary Engineering Division*, 89(2), 31-59, 1963.
- [54] Barka, N., Ouzaouit, K., Abdennouri, M., El Makhfouk, M., Dried prickly pear cactus (*Opuntia ficus indica*) cladodes as a low-cost and eco-friendly biosorbent for dyes removal from aqueous solutions, *Journal of the Taiwan Institute of Chemical Engineers*, 44(1), 52-60, 2013.
- [55] Tsibranska, Hristova, E., Comparison of different kinetic models for adsorption of heavy metals onto activated carbon from apricot stones, *Bulgarian Chemical Communications*, 43(3), 370-377, 2001.
- [56] Anitha, T., Kumar, P., Kumar, K., Ramkumar, B., Ramalingam, S., Adsorptive removal of Pb(II) ions from polluted water by newly synthesized chitosan-polyacrylonitrile blend: Equilibrium, kinetic, mechanism and thermodynamic approach, *Process Safety and Environmental Protection*, 98, 187-197, 2015.